

Structural Requirements for Mitomycin C DNA Bonding[†]Ven-Shun Li,[‡] Daeock Choi,[‡] Moon-shong Tang,^{*,§} and Harold Kohn^{*,‡}

Department of Chemistry, University of Houston, Houston, Texas 77204-5641, and The University of Texas System, M. D. Anderson Cancer Center, Science Park-Research Division, Smithville, Texas 78957

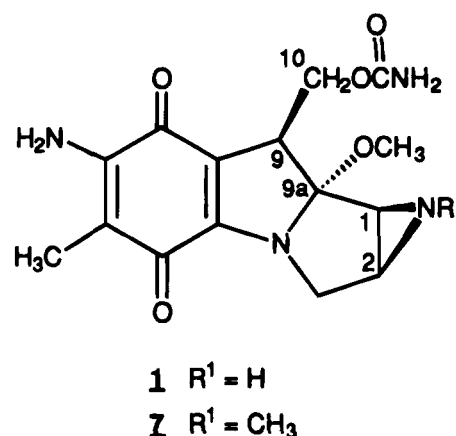
Received January 12, 1995; Revised Manuscript Received March 22, 1995[®]

ABSTRACT: Information of the specific structure of the activated mitomycin species leading to selective DNA bonding has been secured by determining the bonding sequence selectivities of modified mitomycins in which the identity, spatial orientation, and state of unsaturation of the C-9 and C-9a substituents in the mitomycin were varied. Both mitomycin-9a-sulfonate (**8**) and mitomycin D (**9**) gave DNA bonding profiles comparable to those obtained for mitomycin C (**1**) under reductive conditions, indicating that neither the stereochemistry of the C-9 and C-9a substituents nor the identity of the leaving group at C-9a influenced the site(s) of DNA bonding. These results indicated that aromatization of the dihydropyrrole ring in mitomycin C precedes DNA binding and mitomycin C-1 bonding.

Mitomycin C (**1**) is an antitumor antibiotic agent of major clinical significance (Carter & Crooke, 1979). Drug function is believed to occur by reductive activation of **1** and DNA bonding (Scheme 1), leading to the disruption of processes necessary for cellular growth and survival (Tomasz, 1994). It has been demonstrated that mitomycin C *monoalkylation* transformations (i.e., **4** → **5**) proceed only at guanine (G*) sites with 5'-CG* dinucleotide sequences being modified at appreciably higher levels than 5'-AG*, 5'-GG*, and 5'-TG* sequences (Li & Kohn, 1991; Kohn et al., 1992b; Kumar et al., 1992) and that mitomycin C DNA *bisalkylation*, inter-strand cross-linking processes (i.e., **5** → **6**) occur within complementary 5'-CG* sequences rather than at 5'-G*C sequences (Teng et al., 1989; Weidner et al., 1990; Borowy-Borowski et al., 1990). Preliminary evidence has been provided that key hydrogen bond interactions exist between the activated drug (e.g., **4**) and the DNA that foster the observed selective DNA bonding (Li & Kohn, 1991; Kohn et al., 1992a,b; Kumar et al., 1992). Further progress has been hampered by the lack of information on the specific structure of the activated drug leading to DNA bonding in both *in vitro* and *in vivo* transformations. In this paper, we demonstrate that aromatization of the dihydropyrrole ring in the mitomycin precedes DNA binding and mitomycin C-1 bonding.

EXPERIMENTAL PROCEDURES

Materials. Mitomycin C (**1**) (pure) was supplied by Bristol-Myers Squibb Co. (Wallingford, CT). 10-Decarbamoylmitomycin C (Kinoshita et al., 1971) (**11**), porfiromycin (Kasai & Kono, 1992) (**7**), mitomycin-9a-sulfonate (Hornemann et al., 1976; Schiltz & Kohn, 1993) (**8**), and 10-decarbamoyl-9-dehydroporfiromycin (Kono et al., 1990) (**10**) were prepared according to previously described methods. Mitomycin D (Kasai & Kono, 1992; Shirahata et



al., 1981) (**9**) was a gift from Dr. M. Kasai (Kyowa Hakko Kogyo Co., Ltd.). Na₂S₂O₄ was purchased from Fisher Scientific Co. Restriction enzymes and DNA polymerase I (Klenow fragment) were obtained from New England BioLabs. NACS Pacs¹ were purchased from Bethesda Research Laboratories. XO, NADH, and all other chemicals and electrophoretic materials were obtained from either Sigma Chemical Co. or Bio-Rad Laboratories. The [α-³²P]-TTP (specific activity approximately 3000 Ci/mmol) was purchased from Du-Pont-New England Nuclear.

DNA Fragments Isolation and ³²P End Labeling. Plasmid pBR322 was purified by cesium chloride density centrifugation and dialyzed extensively against TE buffer (10 mM Tris-HCl, pH 8.0, 1 mM EDTA). The following procedure was utilized for the isolation of the 129 bp fragment with ³²P labeled at one of the 3' ends. The pBR322 plasmid was first digested with *Bst*NI, and the band corresponding to the 1857 bp fragment was isolated from a 1.4% agarose gel and cleaned by passing through a NACS Pac followed by ethanol precipitation. The 1857 bp fragment was labeled at the 3' termini in the presence of [α-³²P]TTP and Klenow fragment

[†] This research was supported by the National Institutes of Health (CA29756 to H.K.; ES03124 to M.-s.T.) and the Robert A. Welch Foundation (E-607 to H.K.).

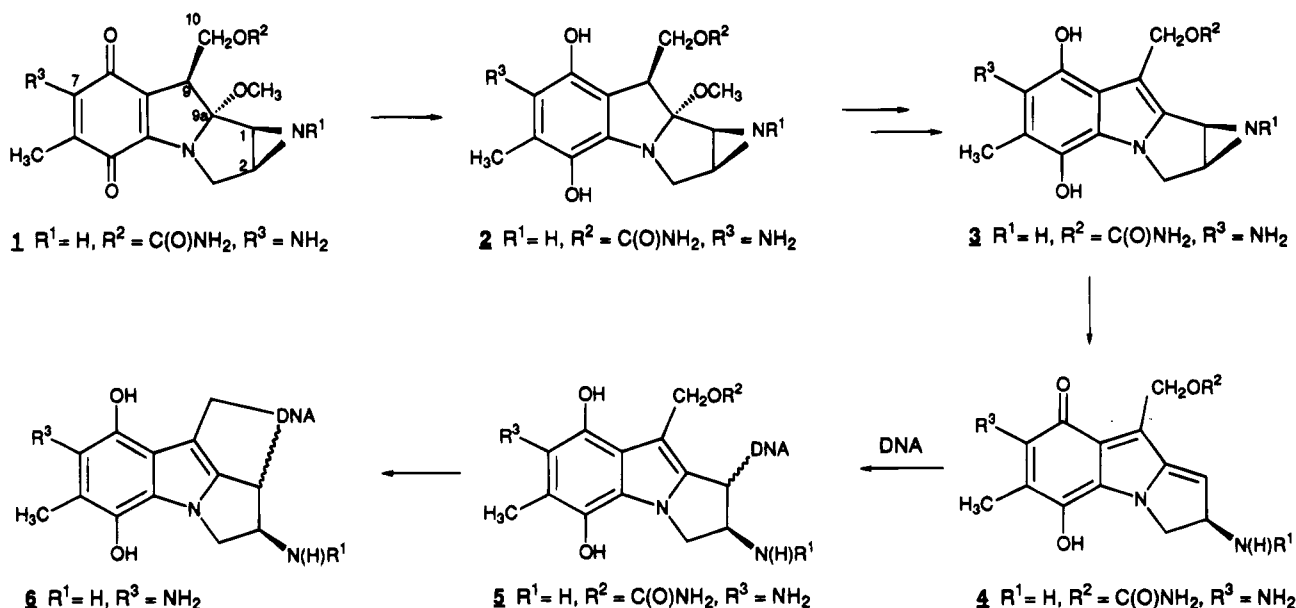
[‡] University of Houston.

[§] The University of Texas System.

[®] Abstract published in *Advance ACS Abstracts*, May 15, 1995.

¹ Abbreviations: NACS pacs, NACS prepacks convertible columns; XO, xanthine oxidase; NADH, nicotinamide adenine dinucleotide, reduced form; TTP, thymidine 5'-triphosphate; TE, Tris-HCl-EDTA; Tris, tris(hydroxymethyl)aminomethane; bp, base pair; DTT, dithiothreitol; EDTA, ethylenediaminetetraacetic acid; ATP, adenosine 5'-triphosphate.

Scheme 1. Proposed Mechanism for the Mode of Action of Mitomycin C



(5 units) in 10 mM Tris-HCl, pH 8.0, 5 mM MgCl₂, and 7.5 mM DTT and incubated at 20 °C (30 min). The labeled DNA fragment was precipitated with ethanol and digested with *Eco*RI. The desired 129 bp fragment was purified by electrophoresis on a 5% polyacrylamide gel.

Drug Bonding with Na₂S₂O₄. DNA–Mitomycin Monoalkylation Reactions. Specified amounts of **1**, **8**, **9**, **10**, and **11** were added to the radiolabeled DNA in 25 mM Tris-HCl buffer, pH 7.4, to give the desired final drug concentration. The solutions were deaerated with Ar (15 min), and then freshly prepared, deaerated, aqueous Na₂S₂O₄ solutions (total 1 equiv) were added in three incremental portions (20 min). The reactions were maintained at 0 or 22 °C (1 h) under Ar and then exposed to air.

Drug Bonding with XO/NADH. DNA–Mitomycin Monoalkylation Reactions. Radiolabeled DNA, drug (**1**, **8**, and **9**), and NADH (2 equiv) were incubated in 100 mM Tris-HCl, pH 7.4, with XO (0.5 unit/μmol of drug) for 20–30 min at 37 °C under Ar and then exposed to air.

Purification of UVRA, UVRB, and UVRC Proteins. UVRA, UVRB, and UVRC proteins were isolated from *Escherichia coli* K12 strain CH296 (*recA*, *endA*/F⁺lacI^Q) carrying plasmids pUNC45 (*uvrA*), pUNC211 (*uvrB*), and pDR3274 (*uvrC*) (Thomas et al., 1985). The methods of purification were the same as described previously (Tang et al., 1991). We term the collective activity of UVRA, UVRB, and UVRC in recognition and incision of modified DNA as UVRABC nuclease.

UVRABC Nuclease Reactions. The UVRABC nuclease reactions were carried out in a reaction mixture (25 μL) containing 50 mM Tris-HCl (pH 7.5), 0.1 mM EDTA, 10 mM MgCl₂, 1 mM ATP, 100 mM KCl, 1 mM DTT, 15 nM UVRA, 15 nM UVRB, 15 nM UVRC, and substrate DNA. The mixtures were incubated at 37 °C (1 h), and the reactions were stopped by phenol–chloroform extractions followed by ethanol precipitation in the presence of aqueous NH₄-OAc (2.5 M). The precipitated DNA was recovered by centrifugation and washed with 80% ethanol.

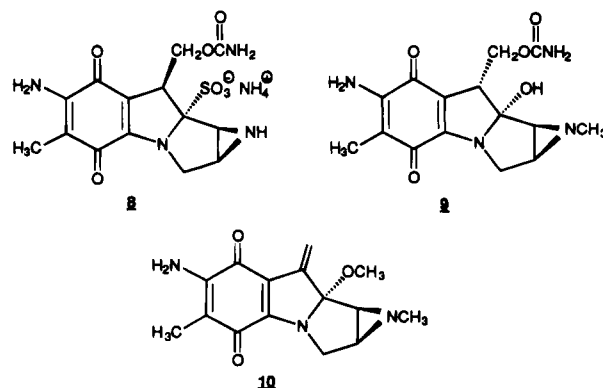
DNA Sequencing, DNA Sequencing Gel Electrophoresis, and Autoradiography. The 3' end ³²P-labeled *Bst*NI–*Eco*RI 129 bp DNA fragment of pBR322 was sequenced by the

method of Maxam and Gilbert (1980). The ³²P-labeled fragments with or without various enzyme treatments were suspended in sequencing tracking dye (80% v/v deionized formamide, 10 mM NaOH, 1 mM EDTA, 0.1% xylene cyanol, and 0.1% bromophenol blue), heated at 90 °C (3 min), and quenched in an ice bath. The samples were applied to a 8% denaturing sequencing gel in parallel with the Maxam and Gilbert sequencing reactions. After electrophoresis the gels were exposed to Kodak X-Omat AR film with intensifying screen at –70 °C.

Densitometric Scanning. The intensities of UVRABC nuclease incision bands were determined with either a Bio-Image Visage 100 System consisting of a high-resolution digitizing camera or a Bio-Image Open Windows Version 3 System consisting of a Howtek Scanmaster 3+ and whole band analysis software.

RESULTS

(A) **The Experimental Design.** In this study, we chose to examine DNA bonding of mitomycin C (**1**) or porfiromycin (*N*-methylmitomycin C) (Kasai & Kono, 1992) (**7**) derivatives modified at the C-9 and C-9a sites. The three compounds evaluated were mitomycin-9a-sulfonate (Hornemann et al., 1976; Schiltz & Kohn, 1993) (**8**), mitomycin D (Kasai & Kono, 1992; Shirahata et al., 1981) (**9**), and 10-decarbamoil-9-dehydroporfiromycin (Kono et al., 1990) (**10**).



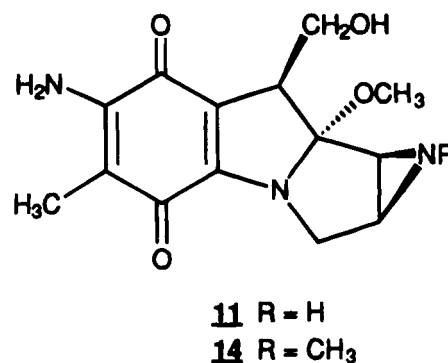
These mitomycins provided information on the importance of the identity, the spatial orientation, and the state of unsaturation of the C-9 and C-9a substituents on DNA bonding sequence specificity.

The selected mitomycins were reductively activated in the presence of DNA, and then their DNA bonding properties were compared to **1**. The 3' end ^{32}P -labeled *Bst*NI–*Eco*RI (upper strand) 129 bp fragment of pBR322 plasmid was used as the test DNA (Li & Kohn, 1991; Kohn et al., 1992a,b). This restriction fragment contained 13 guanine units within the central 67 bp portion of the duplex on the top labeled strand. Embedded in this DNA region are strong (i.e., 5'-CG*T, 5'-CG*C, 5'-TG*T), weak (i.e., 5'-AG*G, 5'-TG*C, 5'-GG*C), and very weak (i.e., 5'-AG*T, 5'-TG*A) affinity mitomycin C trinucleotide bonding sites (Kohn et al., 1992b). The sequence specificity and the degree of drug–DNA bonding were determined by the method of UVRABC nuclease incision analysis (Friedberg, 1984; Sancar & Sancar, 1988; Tang et al., 1988). We previously demonstrated that UVRABC nuclease specifically incises 6–7 bases 5' and 3–4 bases 3' to guanine sites modified by mitomycin C and its derivatives, and that the extent of this enzyme incision is proportional to the concentration of the drug used for DNA modification (Kohn et al., 1992a,b). Therefore, we concluded that the relative intensities of the incision bands generated from the UVRABC treated mitomycin–DNA adducts represented the relative degree of drug modification at each particular guanine residue in the radiolabeled DNA fragment.

In the DNA bonding studies we attempted to activate mitomycins **8**–**10** both enzymatically (XO/NADH) (Kohn et al., 1992a; Phillips et al., 1989; McGuinness et al., 1991) and chemically ($\text{Na}_2\text{S}_2\text{O}_4$) (Li & Kohn, 1991; Schiltz & Kohn, 1993; Tomasz et al., 1974). We incorporated both methods in our experimental design since we have found that not all mitomycins are efficiently activated by XO/NADH. Significantly, we have previously determined that both reductive techniques provided the same DNA bonding profile with mitomycin C (**1**) (Li & Kohn, 1991; Kohn et al., 1992a). The XO/NADH reactions were uniformly run at 37 °C for 20–30 min, while the amount of $\text{Na}_2\text{S}_2\text{O}_4$ (1.0 equiv), the procedure of addition (one, two, or three incremental additions), the temperature of the reaction (0 and 22 °C), and the length of reaction time (1 h) were tailored to the substrate. The $\text{Na}_2\text{S}_2\text{O}_4$ conditions used led to the partial consumption (20–50%) of the starting mitomycin for the corresponding reaction done in the absence of DNA (HPLC analysis).

(B) Mitomycin–DNA Bonding Profiles. The accepted mechanism for mitomycin activation (Scheme 1) proposes that quinone reduction (**1** → **2**) leads to the aromatization of the dihydropyrrole ring (**2** → **3**) (Iyer & Szybalski, 1964; Moore & Czerniak, 1981). Accordingly, neither the initial stereochemistry at C-9 (i.e., **9**) nor the identity of the C-9a leaving group (i.e., **8**, **9**) should influence the sequence selectivity for mitomycin DNA bonding provided binding of the activated mitomycin to the DNA occurs *after* mitosene formation (i.e., **3**). Correspondingly, introduction of an exomethylene group at C-9 in the mitomycin ring skeleton (i.e., **10**) may influence the bonding properties of C-1, as well as influence the relative reactivities of the C-1 and C-10 DNA bonding sites.

Mitomycin-9a-sulfonate (**8**) was activated both enzymatically and chemically. The autoradiogram (Figure 1A) and histograms (Figure 1B) after UVRABC digestion demonstrated that both the DNA bonding sites for **8** (Figure 1A, lanes 7, 8, and 10) and their relative intensities mirrored that of **1** (Figure 1A, lanes 5, 6, and 9) and 10-decarbamoylemitomycin C (Kinoshita et al., 1971) (**11**) (Figure 1A, lanes



11–**13**). Compound **8** proved to be an excellent substrate for XO/NADH. Reductive activation of **8** proceeded at levels comparable to that of **1** in the absence of DNA (HPLC analysis, data not shown). Moreover, both **1** and **8** bound DNA with nearly equal efficiency (gel analysis).

Chemical and enzymatic activation of mitomycin D (**9**) (Figure 2A, lanes 7–9; Figure 2B) also provided a DNA bonding profile similar to that previously observed for mitomycin C (**1**) (Figure 2A, lane 6; Figure 2B). Our finding that less intense radiolabeled DNA bands were observed after UVRABC digestion of the XO/NADH generated products from **9** versus **1** at comparable drug concentrations (Figure 2A, lanes 6, and 7) suggests that enzymatic activation of **9** was less efficient than for **1**. Comparison of the corresponding HPLC data for the XO/NADH reduction of **9** and **1** in the absence of DNA was in agreement with this contention (% activation **1**/ % activation **9** ~5:1, data not shown).

Treatment of 10-decarbamoylemitomycin (**10**) with XO/NADH led to low levels (<3%) of **10** utilization (HPLC analysis). Reductive activation of **10** (0.9 mM) with $\text{Na}_2\text{S}_2\text{O}_4$ (1 equiv) in the presence of DNA followed by UVRABC digestion provided a more complicated DNA cleavage pattern that was different from that of mitomycin C (Kohn et al., 1992b) (data not shown). Correspondingly, treatment of the *Bst*NI–*Eco*RI 129 bp DNA fragment with **10** (1.5 mM) in the *absence* of reductant at 37 °C for 18 h (Figure 3A, lane 5) gave a bonding profile similar to that obtained from **1** (Figure 3A, lane 6), **11** (Figure 1A, lanes 11–13), and **10** (data not shown) under reductive conditions. The intensities of the radiolabeled bands after UVRABC digestion for the DNA sample treated with **10** and XO/NADH were appreciably weaker than those observed for the other experiments despite the high concentration of **10** (1.5 mM) utilized in this reaction. This finding was consistent with the low amounts of **10** consumed upon treatment with XO/NADH (HPLC analysis).

Information on the probable cause for the nonreductive bonding of **10** to DNA was obtained by examining the hydrolysis of 10-decarbamoylemitomycin. Dissolution of **10** (37 °C, 48 h) in an aqueous buffered solution (Tris-HCl, pH 7.4) led to the partial consumption of starting

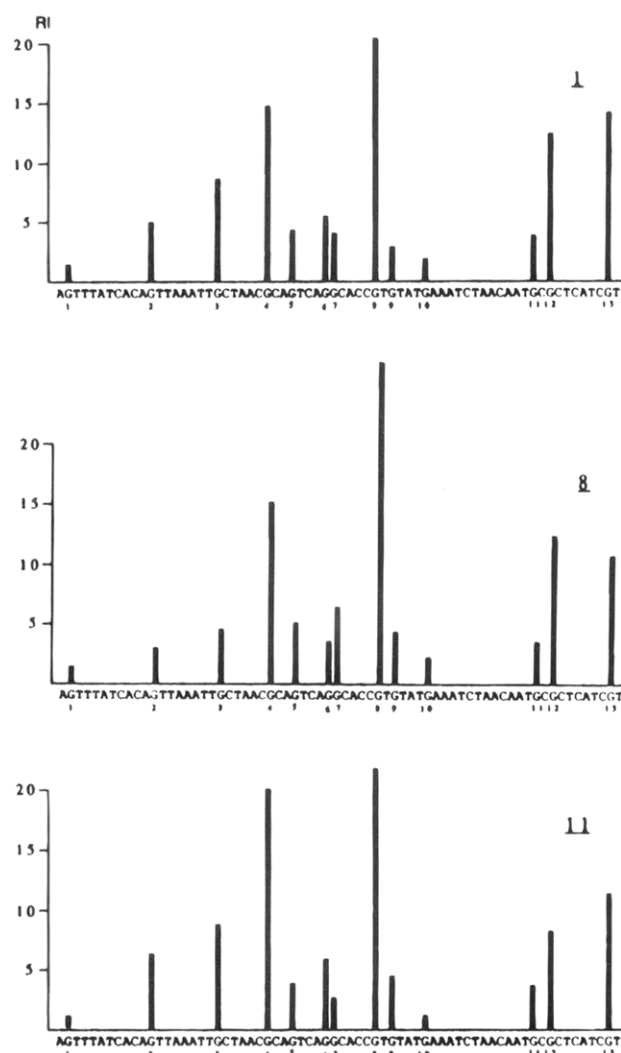
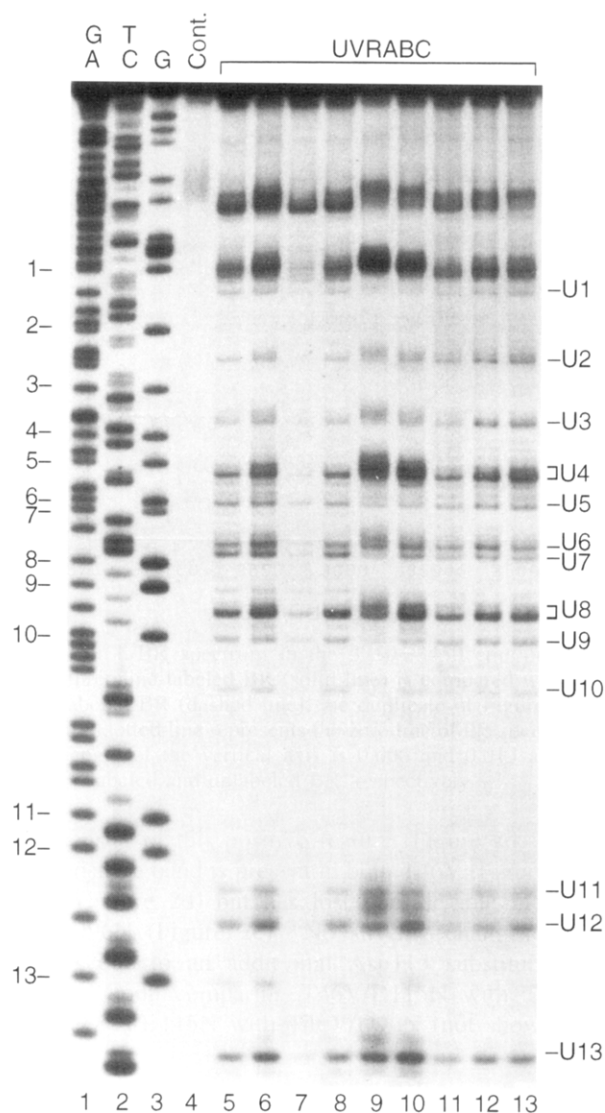
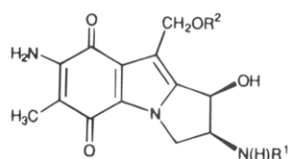
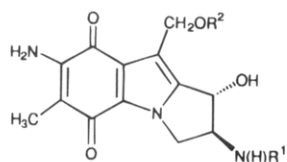


FIGURE 1: (A, left) Autoradiogram of UVRABC nuclease cutting of a mitomycin C (**1**)-modified, mitomycin-9a-sulfonate (**8**)-modified, and 10-decarbomylmitomycin C (**11**)-modified 3' end ^{32}P -labeled *Bst*NI–*Eco*RI 129 bp fragment of pBR322 plasmid (top strand): lanes 1–3, Maxam-Gilbert sequencing reactions of AG, TC, and G, respectively; lane 4, DNA modified with 0.45 mM **1** after reductive activation with $\text{Na}_2\text{S}_2\text{O}_4$ (1 equiv, three incremental additions, 0 °C) without UVRABC cutting (control); lanes 5 and 6, DNA modified with 0.45 and 0.9 mM **1**, respectively, after reductive activation with XO/NADH; lanes 7 and 8, DNA modified with 0.45 and 0.9 mM **8**, respectively, after reductive activation with XO/NADH; lane 9, DNA modified with 0.45 mM **1** after reductive activation with $\text{Na}_2\text{S}_2\text{O}_4$ (1 equiv, three incremental additions, 0 °C); lane 10, DNA modified with 0.45 mM **8** after reductive activation with $\text{Na}_2\text{S}_2\text{O}_4$ (1 equiv, three incremental additions, 0 °C); lane 11, DNA modified with 0.45 mM **11** after reductive activation with $\text{Na}_2\text{S}_2\text{O}_4$ (1 equiv, three incremental additions, 22 °C); lane 12, DNA modified with 0.45 mM **11** after reductive activation with $\text{Na}_2\text{S}_2\text{O}_4$ (1 equiv, three incremental additions, 3% DMSO, 22 °C); lane 13, DNA modified with 0.45 mM **11** after reductive activation with $\text{Na}_2\text{S}_2\text{O}_4$ (1 equiv, added all at once, 22 °C). The drug modification induced UVRABC nuclease incision bands (U1–U13) are labeled on the right side of the panel, and the numbers correspond to the guanine residues (1–13) that are numbered on the left side of the panel. (B, right) Relative intensities (RI) of UVRABC nuclease incision of mitomycin **1**–, **8**–, and **11**–DNA adducts of 67 base region within 3' end ^{32}P -labeled *Bst*NI–*Eco*RI 129 bp sequence from pBR322 plasmid. The concentration was 0.9 mM for **1** and **8** (XO/NADH) and 0.45 mM for **11** ($\text{Na}_2\text{S}_2\text{O}_4$). U1–U13 bands in lanes 6, 8, and 11 of panel A were scanned by a densitometer, and the relative intensity of each band is plotted at the corresponding G in the sequence.

material (5%) and the appearance of two new peaks that corresponded to *cis*-(**12**) and *trans*-1,10-dihydroxy-7-amino-2-*N*-methylaminomitosenes (**13**) (Han et al., 1992) (HPLC analysis).



12 R¹ = CH₃, R² = H
17 R¹ = H, R² = C(O)NH₂



13 R¹ = CH₃, R² = H
18 R¹ = H, R² = C(O)NH₂

The identities of **12** and **13** were verified by coinjection of authentic samples of these adducts with the reaction mixture. Significantly, **14** was not observed by HPLC analysis. This result suggested that the activated species responsible for the UVRABC DNA digestion pattern in the reaction conducted in the absence of reductant was **15**. We have previously shown that 7-aminoaziridinomitosenes (**16**) efficiently modified DNA at low mitomycin concentrations and that the UVRABC digestion profiles for **16**-modified DNA and reductively activated mitomycin C were the same (Kohn et al., 1992b). Furthermore, compound **16** underwent rapid hydrolysis to **17** and **18** in neutral and acidic solutions (Han & Kohn, 1991).

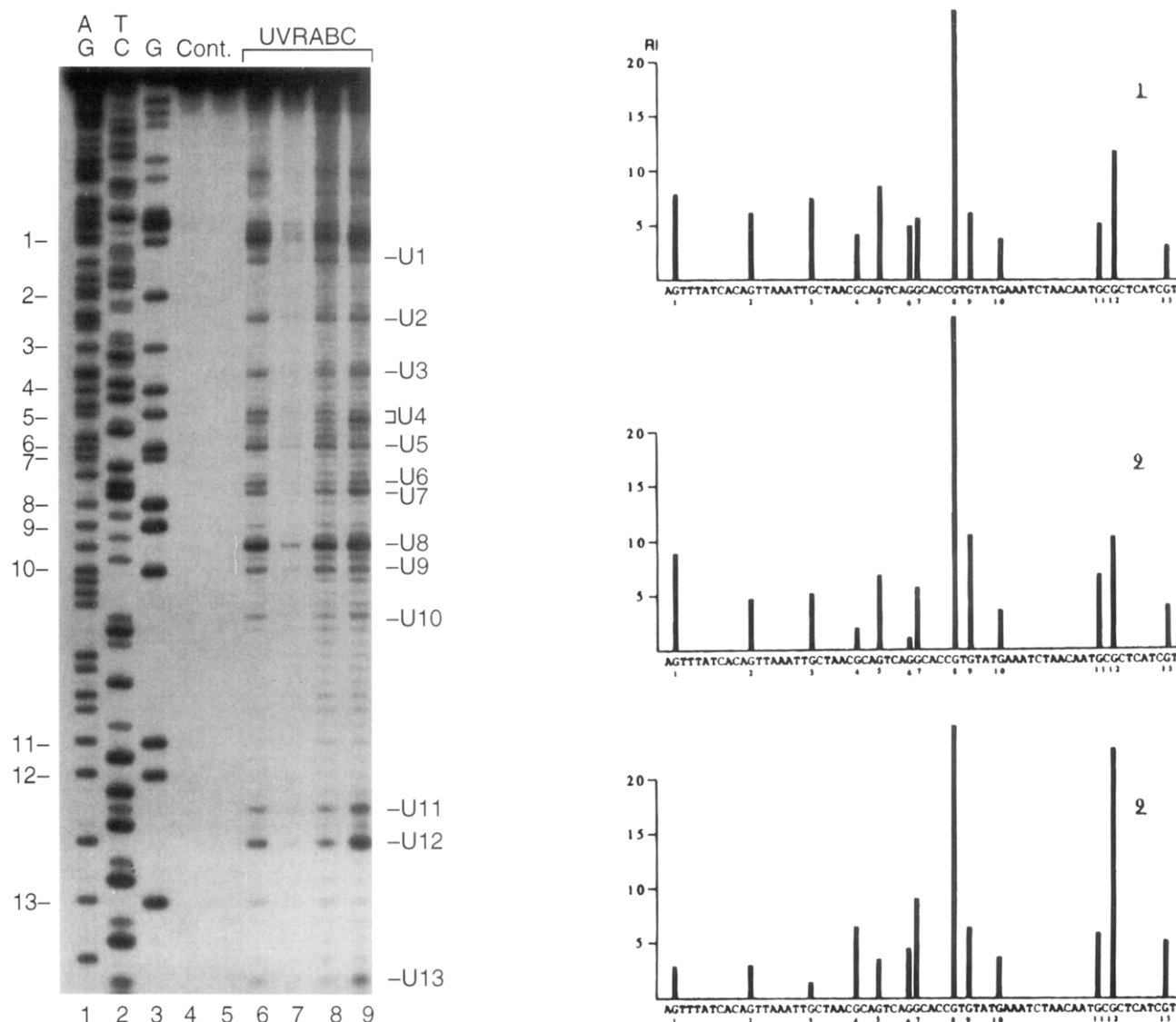
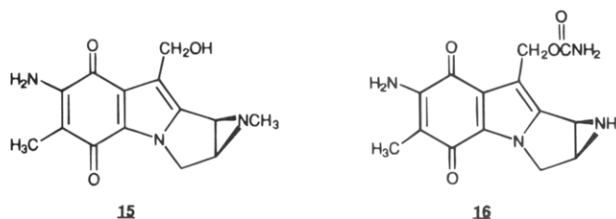


FIGURE 2: (A, left) Autoradiogram of UVRABC nuclease cutting of a mitomycin C (**1**)-modified and mitomycin D (**9**)-modified 3' end ^{32}P -labeled *Bst*NI-*Eco*RI 129 bp fragment of pBR322 plasmid (top strand): lanes 1-3, Maxam-Gilbert sequencing reactions of AG, TC, and G, respectively; lane 4, DNA modified with 0.9 mM **9** after reductive activation with XO/NADH without UVRABC cutting (control); lane 5, native DNA without UVRABC cutting (control); lane 6, DNA modified with 0.9 mM **1** after reductive activation with XO/NADH; lanes 7 and 8, DNA modified with 0.9 and 1.5 mM **9**, respectively, after reductive activation with XO/NADH; lane 9, DNA modified with 0.3 mM **9** after reductive activation with $\text{Na}_2\text{S}_2\text{O}_4$ (1 equiv, three incremental additions, 22 °C). The drug modification induced UVRABC nuclease incision bands (U1-U13) are labeled on the right side of the panel, and the numbers correspond to the guanine residues (1-13) that are numbered on the left side of the panel. (B, right) Relative intensities (RI) of UVRABC nuclease incision of mitomycin **1**- and **9**-DNA adducts of 67 base region within 3' end ^{32}P -labeled *Bst*NI-*Eco*RI 129 bp sequence from pBR322 plasmid. The concentration was 0.9 mM for **1** (XO/NADH), 1.5 mM for **9** (XO/NADH), and 0.3 mM for **9** ($\text{Na}_2\text{S}_2\text{O}_4$). U1-U13 bands in lanes 6, 8, and 9 of panel A were scanned by a densitometer, and the relative intensity of each band is plotted at the corresponding G in the sequence.



A potential pathway for the conversion of **10** to **15** and then to **12** and **13** is presented in Scheme 2. Conjugate addition of water to **10** gives **19**, which undergoes acid-catalyzed conversion (McClelland & Lam, 1985) to mitosene **15**. Aziridine protonation followed by $\text{S}_{\text{N}}1$ ring opening and reaction with water then gives **12** and **13**. We suspect that a similar nucleophile-initiated pathway may be operative in the $\text{Na}_2\text{S}_2\text{O}_4$ -mediated reactions and that the conversion of

10 to **15** or comparable intermediate may be facilitated by the reductant. The mechanism of this reductive process is under investigation.

DISCUSSION

Iyer and Szybalski (1964) suggested the first mechanism for the mode of action of mitomycin C. This hypothesis was subsequently modified by Moore in 1981 to include quinone methide **4** (Scheme 1) (Moore & Czerniak, 1981). These proposals have led to detailed mechanistic studies that have yielded a clearer molecular description of the sequential chemical transformations that lead to drug activation and have provided general support for Iyer and Szybalski's prescient hypothesis. However, information on the specific structure of the activated mitomycin species that binds to DNA prior to bonding is still lacking. In this study, we have

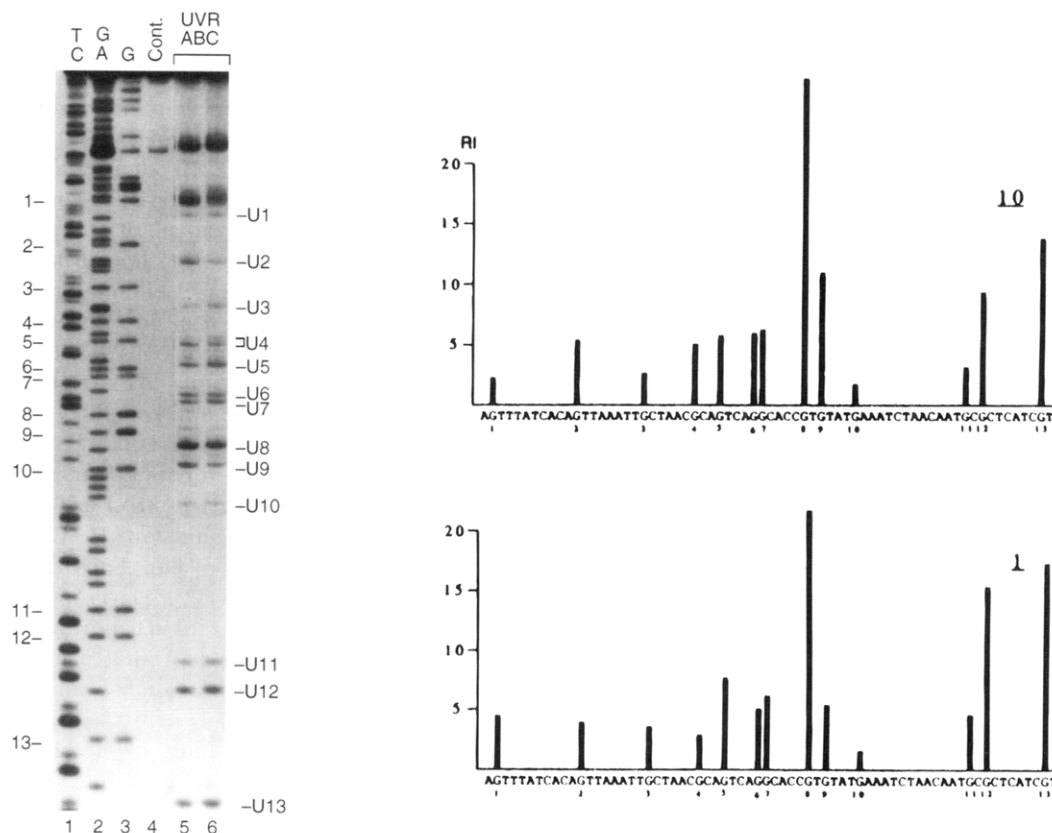
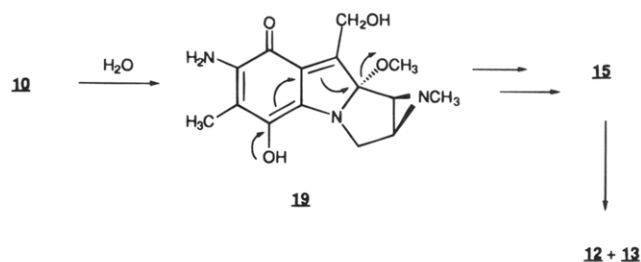


FIGURE 3: (A, left) Autoradiogram of UVRABC nuclease cutting of a mitomycin C (**1**)-modified and 10-decarbamoyl-9-dehydroporfiromycin (**10**)-modified 3' end ^{32}P -labeled *Bst*NI-*Eco*RI 129 bp fragment of pBR322 plasmid (top strand): lanes 1–3, Maxam–Gilbert sequencing reactions of TC, AG, and G, respectively; lane 4, native DNA without UVRABC cutting (control); lane 5, DNA modified with 1.5 mM **10** after incubated at 37 °C for 18 h; lane 6, DNA modified with 0.9 mM **1** after reductive activation with XO/NADH. The drug modification induced UVRABC nuclease incision bands (U1–U13) are labeled on the right side of the panel, and the numbers correspond to the guanine residues (1–13) that are numbered on the left side of the panel. (B, right) Relative intensities (RI) of UVRABC nuclease incision of mitomycin **10**– and **1**–DNA adducts of 67 base region within 3' end ^{32}P -labeled *Bst*NI-*Eco*RI 129 bp sequence from pBR322 plasmid. The concentration was 1.5 mM for **10** (37 °C, 18 h) and 0.9 mM for **1** (XO/NADH). U1–U13 bands in lanes 5 and 6 of panel A were scanned by a densitometer, and the relative intensity of each band is plotted at the corresponding G in the sequence.

Scheme 2. Proposed Pathway for Hydrolysis of **10**



examined the effect of the C-9 and C-9a mitomycin substituents on the drug–DNA interaction process. Both mitomycin-9a-sulfonate (**8**) and mitomycin D (**9**) gave nearly identical DNA bonding profiles as mitomycin C (Figures 1, and 2). These findings indicated that quinone reduction and aromatization of the dihydropyrrole preceded DNA binding and C-1 bonding and implied that neither the stereochemistry of the C-9 and C-9a substituents nor the identity of the leaving group at C-9a influenced the site(s) of DNA bonding. Significantly, if aromatization of the dihydropyrrole ring in **8** had not occurred prior to mitomycin–DNA complexation, then in the proposed alignment of the activated mitomycin with DNA (Kohn et al., 1992b; Kumar et al., 1992) the C-9a sulfonate substituent would be directed toward the floor of the minor groove. We suspect that this interaction would significantly perturb the sequence selectivity for **8** DNA bonding. The proposed pathway for mitomycin C binding

and C-1 bonding is supported by the finding that the DNA bonding profile for the aromatic mitosene **16** under nonreductive conditions was virtually identical to that of reductively activated **1** (Kohn et al., 1992b).

Information of the specific oxidation state of the quinone ring in the activated mitosene (i.e., **3** and **16**) that preceded DNA binding and bonding was not deduced from these experiments. We have previously shown that substantial amounts of **1** as well as **8** remained after reductive activation of each of these mitomycins (Schiltz & Kohn, 1993) and have provided evidence along with other investigators that the unreacted mitomycin in solution can disproportionate with 7-aminoaziridinoleucomitosene (**3**) to give the leucomitosene (i.e., **2**) and 7-aminoaziridinomitosenes (**16**) (Schiltz & Kohn, 1993; Pan et al., 1984; Hoey et al., 1988; Machtalere et al., 1988). Since compound **16** bonds to DNA in sequence selective manner identical to that observed for **1** under reductive conditions (Kohn et al., 1992b), we are unable to assign whether the activated mitosene that alkylates DNA is in the reduced or oxidized state.

The combined findings for **8** and **9** on mitomycin DNA bonding have provided an intriguing picture of the nature of the reactive intermediate that leads to the drug–DNA covalent monoadduct **5**. The near identity of the bonding profiles for mitomycin C (**1**), mitomycin C-9a-sulfonate (**8**), and mitomycin D (**9**) suggests that quinone reduction followed by the stepwise aromatization of the dihydropyrrole

ring precede the initial complexation of the activated mitomycin with the DNA. The importance of the C-7, C-10, and N(1a) sites in mitomycin C on C-1 DNA bonding are currently being evaluated.

ACKNOWLEDGMENTS

We thank Ms. A. Pao and Mr. X. Ye for UVR protein purification, Mr. Y. Zheng for DNA purification, and Dr. A. Sancar (University of North Carolina—Chapel Hill) for providing *E. coli* strains containing UVR gene plasmids. Grateful acknowledgment is made to Drs. A. M. Casazza and W. Rose and the Bristol-Myers Squibb Co. (Wallingford, CT) for the generous gift of mitomycin C and Dr. M. Kasai and Kyowa Hakko Kogyo Co., Ltd. for providing us with mitomycin D (9).

REFERENCES

- Borowy-Borowski, H., Lipman, R., & Tomasz, M. (1990) *Biochemistry* 29, 2999–3006.
- Carter, S. K., & Crooke, S. T. (1979) *Mitomycin C. Current Status and New Developments*, Academic Press, New York.
- Friedberg, E. C. (1984) *DNA Repair*, W. H. Freeman, New York.
- Han, I., & Kohn, H. (1991) *J. Org. Chem.* 56, 4648–4653.
- Han, I., Russell, D. J., & Kohn, H. (1992) *J. Org. Chem.* 57, 1799–1807.
- Hoey, B. M., Butler, J., & Swallow, A. J. (1988) *Biochemistry* 27, 2608–2614.
- Hornemann, U., Ho, Y.-K., Mackey, J. K., Jr., & Srivastava, S. C. (1976) *J. Am. Chem. Soc.* 98, 7069–7074.
- Iyer, V. N., & Szybalski, W. (1964) *Science* 145, 55–58.
- Kasai, M., & Kono, M. (1992) *Synlett.* 778–790.
- Kinoshita, S., Uzu, K., Nakano, K., & Takahashi, T. (1971) *J. Med. Chem.* 14, 109–112.
- Kohn, H., Li, V.-S., Schiltz, P., & Tang, M.-s. (1992a) *J. Am. Chem. Soc.* 114, 9218–9220.
- Kohn, H., Li, V.-S., & Tang, M.-s. (1992b) *J. Am. Chem. Soc.* 114, 5501–5509.
- Kono, M., Kasai, M., & Shirahata, K. (1990) *J. Antibiot.* 43, 383–390.
- Kumar, S., Lipman, R., & Tomasz, M. (1992) *Biochemistry* 31, 1399–1407.
- Li, V.-S., & Kohn, H. (1991) *J. Am. Chem. Soc.* 113, 275–283.
- McClelland, R. A., & Lam, K. (1985) *J. Am. Chem. Soc.* 107, 5182–5186.
- McGuinness, B. F., Lipman, R., Goldstein, J., Nakanishi, K., & Tomasz, M. (1991) *Biochemistry* 30, 6444–6453.
- Machtalere, G., Houee-Levin, C., Gardes-Albert, M., Ferradini, C., & Hickel, B. (1988) *C. R. Acad. Sci. Ser.* 2 307, 17–22.
- Maxam, A., & Gilbert, W. (1980) *Methods Enzymol.* 65, 499–560.
- Moore, H. W., & Czerniak, R. (1981) *Med. Res. Rev.* 1, 249–280.
- Pan, S.-S., Andrews, P. A., Glover, C. J., & Bachur, N. R. (1984) *J. Biol. Chem.* 259, 959–966.
- Phillips, D. R., White, R. J., & Cullinane, C. (1989) *FEBS Lett.* 246, 233–240.
- Sancar, A., & Sancar, G. B. (1988) *Annu. Rev. Biochem.* 57, 29–67.
- Schiltz, P., & Kohn, H. (1993) *J. Am. Chem. Soc.* 115, 10497–10509.
- Shirahata, K., Morimoto, M., Ashizawa, T., Mineura, K., Kono, M., Saitoh, Y., & Kasai, M. (1981) The 21st Interscience Conference on Antimicrobial Agents and Chemotherapy, Chicago, Nov 1981, Abstracts, p 421.
- Tang, M.-s., Lee, C.-S., Doisy, R., Ross, L., Needham-VanDevanter, D. R., & Hurley, L. H. (1988) *Biochemistry* 27, 893–901.
- Tang, M.-s., Nazimiec, M. R., Doisy, R. P., Pierce, J. R., Hurley, L. H., & Alderete, B. E. (1991) *J. Mol. Biol.* 220, 855–866.
- Teng, S. P., Woodson, S. A., & Crothers, D. M. (1989) *Biochemistry* 28, 3901–3907.
- Thomas, D. C., Levy, M., & Sancar, A. (1985) *J. Biol. Chem.* 260, 9875–9883.
- Tomasz, M. (1994) in *Molecular Aspects of Anticancer Drug—DNA Interactions* (Neidle, S., & Waring, M., Eds.) Vol. 2, pp 312–348, Macmillan, Boca Raton, FL.
- Tomasz, M., Mercado, C. M., Olson, J., & Chatterjee, N. (1974) *Biochemistry* 13, 4878–4887.
- Weidner, M. F., Signurdsson, S. T., & Hopkins, P. B. (1990) *Biochemistry* 29, 9225–9233.

BI950083+